Impact of Micro-Porous Layer Cracks Morphology on Two-Phase Behaviors in Proton Exchange Membrane Fuel Cell

Xin Shi, Daokuan Jiao, Qing Du, Kui Jiao*

State Key Laboratory of Engines, Tianjin University, 135 Yaguan Rd, Tianjin, China, 300350
*Corresponding author: kjiao@tju.edu.cn;

ABSTRACT

Recently, it is found that cracks are generated on the micro-porous layer (MPL) surface during the fabrication, and these cracks may act as the main transport paths for liquid water to enter the gas diffusion layer (GDL) from the catalyst layer. In this study, the effects of MPL cracks on liquid behavior in GDL were investigated through a three-dimensional two-phase volume-of-fluid model with reconstructed fibrous structure. Meanwhile, the overlap structure of MPL and GDL fiber was considered in this study. The results showed that the overlap between the cracks and the GDL fibers had a significant influence on the formation of the liquid water breakthrough path. In contrast, cracks shape had less influence on the two-phase flow.

Keywords: proton exchange membrane fuel cell; micro-porous layers; volume-of-fluid model; two-phase transport

INTRODUCTION

In recent years, proton exchange membrane (PEM) fuel cells have attracted much attention due to the high conversion efficiency, zero emissions, and quick start-up. PEM fuel cells convert the chemical energy into electrical energy through the electrochemical reaction of hydrogen and oxygen, and produce pure water [1]. Excessive product water in GDL may block the gas diffusion pathway and result in severe water flooding, but the membrane humidity should also be maintained to avoid a low ion conductivity. Thus, the improvement of water management in GDL is becoming crucial. With the global commercialization of fuel cell products, the higher power density requires a higher reactant supply speed and product transport efficiency.

At present, experimental method is often utilized to investigate GDL related issues. Flückiger et al. [2] used an X-ray tomography microscope to observe the process of liquid water intrusion and breakthrough in the ex-situ GDL under different pressures, and obtained 3D water distribution images. The local saturation as a function of capillary pressure was also measured. However, their research did not consider MPL structure. When MPL is applied on GDL, the pore size, permeability, thickness, etc., can exhibits significant differences. Deevanhxay et al. [3] used soft X-ray technology to observe in-situ GDL with and without MPL. The results showed that the addition of MPL reduces the accumulation of liquid water at the CL/GDL interface, making the cell performance better than that without MPL.

However, considering the high cost brought by the high-resolution observation equipment, numerical methods could have several superiorities for the study two-phase flows in GDL and MPL [1]. Gostick et al. [4] combined experimental and numerical methods to investigate the functional relationship between capillary pressure and liquid water saturation in GDL. Through the pore network (PN) model calculation, it was found that the water saturation was greatly reduced after the addition of MPL, which was consistent with the experimental results. They also pointed out that condensation was not the main way of water accumulation in GDL.

Due to the huge modeling scale difference between MPL and GDL, it's extremely difficult to satisfy the computational requirements when coupling them together at the same time. So the MPL was simply to cracks and considered as the water transport paths in numerical studies. Deng et al. [5] employed the stochastic method to reconstruct the 3D structure of

MPL and GDL. Using a mesoscopic lattice Boltzmann (LB) model, they investigated the influence of spatial distribution of PTFE in GDL when coupled MPL cracks on the distribution of liquid water in GDL. The results showed that the uniform distribution PTFE can accelerate the liquid water permeation in GDL, and MPL can relieve water flooding and gather liquid water around cracks to improve the transportation of gas reactants. Their model did not take into account the contact interface of MPL/GDL and the shape of cracks.

So, in this work, considering the overlap of the two layers, a 3D GDL/MPL model was reconstructed which is close to the realistic structures. And the influence of overlapping thickness, cracks shape, GDL substrate porosities on the distribution of liquid water in GDL was investigated.

1. NUMERICAL METHODS

1.1 Governing equations

In this study, the volume-of-fluid (VOF) method was adopted. In VOF model, phase fraction α is solved in each cell to track the interface. When α is 0, the cell is filled with air, while $\alpha=1$ denotes full liquid and α 0 to 1 represents gas-liquid interface. The governing equations are as follows:

$$\nabla \cdot \vec{U} = 0 \tag{1}$$

$$\frac{\partial \alpha}{\partial t} + \nabla \cdot \alpha\vec{U} + \nabla \cdot \left[\alpha(1-\alpha)\vec{U_r}\right] = 0 \tag{2}$$

$$\frac{\partial}{\partial t}(\rho\vec{U}) + \nabla \cdot (\rho\vec{U}\vec{U}) - \nabla \cdot (\mu\nabla\vec{U}) - (\nabla\vec{U}) \cdot \nabla\mu = -\nabla p_d - \vec{g} \cdot \vec{x}\nabla\rho + \sigma\kappa\nabla\alpha \tag{3}$$

$$\rho = \rho_l\alpha + \rho_g(1-\alpha) \tag{4}$$

$$\mu = \mu_l\alpha + \mu_g(1-\alpha) \tag{5}$$

$$\kappa = -\nabla \cdot (\vec{n_w}\cos\theta + \vec{t_w}\sin\theta) \tag{6}$$

The mass conservation equation, the phase conservation equation and the momentum equation are equations 1-3, where σ, κ, μ, represents the surface tension coefficient, the average curvature of the phase interface, and the dynamic viscosity. $\vec{U_r}$ represents the relative velocity of liquid and gas at the interface, i.e. $\vec{U_l} - \vec{U_g}$. The subscripts "l" and "g" refer to "liquid" and "gas" respectively. $\vec{n_w}$ is the unit vector perpendicular to the wall and $\vec{t_w}$ is the unit vector tangent to the wall. θ represents static surface contact angle. To simplify the boundary conditions, the modified pressure is defined as $p_d = p - \rho\vec{g} \cdot \vec{x}$, where $\vec{x}$ is the position vector and $\vec{g}$ is the gravity vector.

1.2 Computational domain

Fig. 1(a) shows the computational domain of GDL and MPL, which has a thickness of 111 μm, a cross-sectional dimension of 200 μm*200 μm, and a fiber diameter of 8 μm. Constant velocity boundary and pressure outlet boundary are adopted for the inlet and outlet, respectively. Corresponding with the generally used pressure ranging from 1000-6000 Pa, the average water velocity in the thickness direction of the GDL ranges from 0 to 0.014m/s [6], and thus the inlet velocity is set to 0.005m/s. The pressure at the outlet is 0 (1 atm) and the pressure boundary for side walls is zero-in-gradient. In addition, according to the measured contact angle of the PTFE material surface, a static contact angle of the fiber surface and the crack wall surface is set to 109° [6].

The computational domain of GDL and MPL are
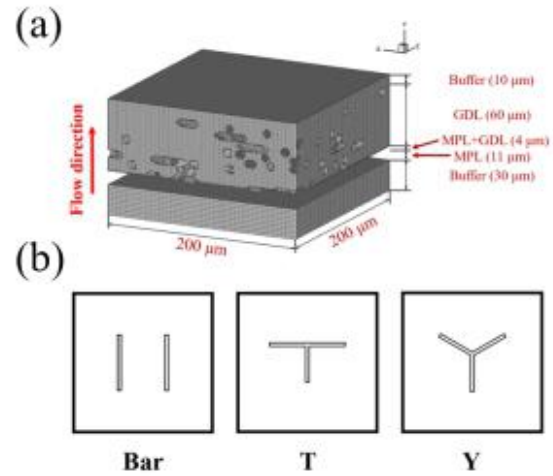
Fig 1 Reconstruction of GDL and MPL (a) Fluid computational domain of GDL coupled MPL, (b) Shape designs of the MPL cracks.

spatially discretized by 2*2*2 and 2*2*1 μm³ hexahedral grids, respectively, which is proved reasonable in previous literature [6]. The entire calculation process of the numerical simulation is completed using the two-phase solver interFoam in the open source platform OpenFOAM. To ensure numerical stability and computational efficiency, the Courant number is limited to less than 0.4.

2. RESULTS AND DISCUSSION

In this study, a model of MPL coupled with GDL is used to investigate the behavior of liquid water. The MPL is reconstructed into two bar-shaped cracks, as shown in Fig. 1. Two liquid water intruding ways into the GDL are observed.

The upper four figures of Fig. 2 show that liquid water enters the GDL only through one of the cracks. The water cluster breakthrough in GDL with a stable transport channel; the lower four figures show that liquid water enters the GDL along two both cracks, two clusters form and continue to expand. When the length of the cluster grows comparable to the thickness of GDL, breakthrough occurs and liquid water emerges, and then the water channel is closed. Similar phenomena are observed in another cluster, and the two clusters alternately break through. In this condition, the drainage process of GDL is intermittent.
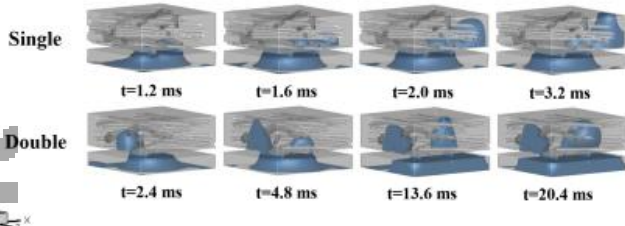
Fig 2 Processes of liquid water intruding into the GDL, single means water forms a channel through only one crack, double means water enters GDL through two cracks.

Fig. 3 describes the difference in cross-section of liquid water caused by MPL cracks. In the realistic structure, MPL and GDL are intertwined with each other, and there are overlapping parts. This detail is not taken into account in the previous simulation. In this model, there is an overlap of 4 µm between MPL and GDL, which is a radius of the fiber. Fig. 3(a) shows the distribution of liquid water at the interface between GDL and MPL. Fig. 3(b) shows the number of grids of cracks, a, b, c, d refers to the four cracks from left to right in Fig. 3(a). It represents the relative relationship between cracks and fibers. The crack with a small number of grids indicate that the crack is located on fibers and has a large overlapping volume, while the crack with a large number of grids indicate that it has
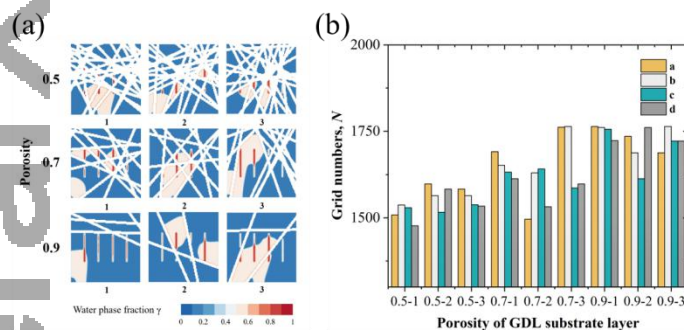
Fig 3 (a) Water distribution at GDL/MPL interface and (b) Grid numbers of MPL cracks.

less contact with fibers or has a small overlapping part. We can see that liquid water is more inclined to choose MPL cracks that have less contact with fibers as paths. This may be due to the larger pores above the crack that overlaps less with GDL fibers, which means smaller capillary pressure. It is easier for water to select this location as the initial entryway. This is significant for a structure design of an orderly GDL. Especially the design of the fiber porosity and position at the GDL/MPL interface.

Considering that high-temperature sintering is required in the process of MPL fabricating, cracks are generated in the process due to constrained drying, which is similar to the process of mud crack [9,10]. According to the formation conditions of mud cracks, the proportion of the shape of MPL cracks can be controlled during the fabrication of MPL. In conclusion, three crack shapes have been designed, which are type-Bar, type-T and type-Y as shown in the Fig. 1(b).
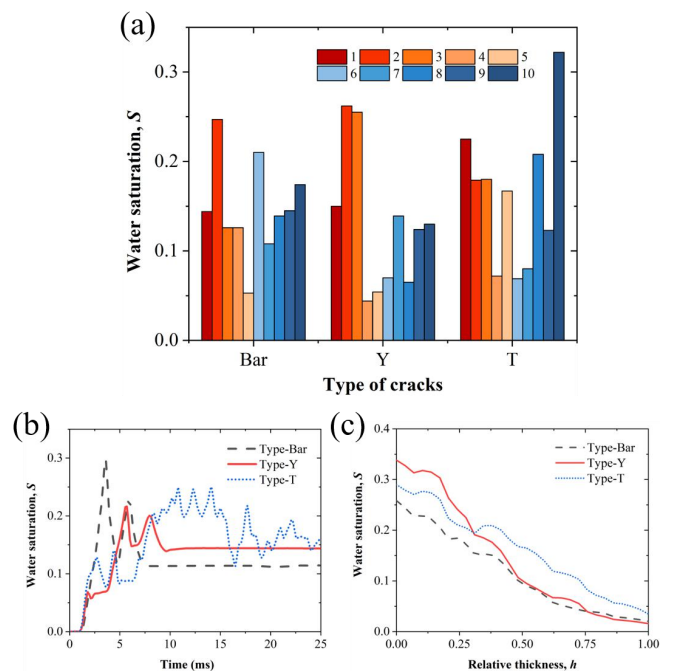
Fig 4 Influence of types of crack on water transport in GDL (a) water saturation of GDL in 3 types of crack, (b) comparisons of 3 types of crack water saturation along the time, (c) comparisons of 3 types of crack water saturation along the through-plane direction for GDL.

Fig. 4(a) shows the liquid water saturation of three crack shapes in 10 sets of GDL structures with a porosity of 0.8. There does not seem to be a significant relationship between crack shape and liquid water saturation. But it is worth noting that in the examples of type-Bar and type-Y cracks, liquid water enters the accumulation stage after entering GDL. Water

saturation increases rapidly until it reaches its peak, and the water clusters break through. A stable water transport channel is formed, and stable breakthrough paths are observed. On the contrary, the GDL coupled with type-T cracks has different drainage rules. It can be seen that the S-T curve has been fluctuating and cannot reach stability. The liquid water presents a cycle of accumulation-breakthrough-drainage. Fluctuating drainage cycle is identified. However, the results of multiple examples showed that this phenomenon is not specific in type-T cracks. Similar phenomena have been observed in other crack shapes. The bottom group of results in Fig. 2 shows a similar process. Fig. (c) shows the change in water saturation along the thickness direction. The water saturation decreases uniformly along the thickness direction, which is consistent with the uniform porosity of the model.

3. CONCLUSION

The influence of overlap between gas diffusion layer (GDL) and micro-porous layer (MPL) on the two-phase flow in GDL was originally considered. It is found that the overlap volume between the cracks and fibers affects the preferred liquid transport pathways. The liquid water is more inclined to emerge from the cracks with less overlap with fibers. Besides, with the reconstruction of different MPL cracks, it is found that the cracks shape has less significant effect on the water transport in GDL. In addition, two special GDL drainage ways were distinguished, namely, single path drainage and multiple path drainage. For single path drainage, the water channel in the GDL is relatively stable. While for multiple path drainage, circulating drainage could result in an unstable water channel.

REFERENCE

[1] Jiao D, Jiao K, Du Q. Two-Phase Flow in Porous Electrodes of Proton Exchange Membrane Fuel Cell. Transactions of Tianjin University, 2020: 1-11.
[2] Flückiger R, Marone F, Stampanoni M, et al. Investigation of liquid water in gas diffusion layers of polymer electrolyte fuel cells using X-ray tomographic microscopy. Electrochimica Acta, 2011, 56(5): 2254-2262.
[3] Deevanhxay P, Sasabe T, Tsushima S, et al. Effect of liquid water distribution in gas diffusion media with and without microporous layer on PEM fuel cell performance. Electrochemistry Communications, 2013, 34: 239-241.
[4] Gostick J T, Ioannidis M A, Pritzker M D, et al. Impact of liquid water on reactant mass transfer in PEM fuel cell electrodes. Journal of the Electrochemical Society, 2010, 157(4): B563.
[5] Deng H, Hou Y, Jiao K. Lattice Boltzmann simulation of liquid water transport inside and at interface of gas diffusion and micro-porous layers of PEM fuel cells. International Journal of Heat and Mass Transfer, 2019, 140: 1074-1090.
[6] Niu Z, Wang Y, Jiao K, et al. Two-phase flow dynamics in the gas diffusion layer of proton exchange membrane fuel cells: volume of fluid modeling and comparison with experiment. Journal of The Electrochemical Society, 2018, 165(9): F613.
[7] Niu Z, Bao Z, Wu J, et al. Two-phase flow in the mixed-wettability gas diffusion layer of proton exchange membrane fuel cells. Applied Energy, 2018, 232: 443-450.
[8] Sasabe T, Deevanhxay P, Tsushima S, et al. Soft X-ray visualization of the liquid water transport within the cracks of micro porous layer in PEMFC. Electrochemistry Communications, 2011, 13(6): 638-641.
[9] Ma J, Zhang X, Jiang Z, et al. Flow properties of an intact MPL from nano-tomography and pore network modelling. Fuel, 2014, 136: 307-315.
[10] Zhao Z, Guo Y, Yan W, et al. Growth patterns and dynamics of mud cracks at different diagenetic stages and its geological significance. International Journal of Sediment Research, 2014, 29(1): 82-98.